

Thermal conductance and electron-phonon coupling in mechanically suspended nanostructures

C. S. Yung, D. R. Schmidt, and A. N. Cleland^{a)}

Department of Physics and iQUEST, University of California at Santa Barbara, Santa Barbara, California 93106

(Received 18 February 2002; accepted for publication 9 May 2002)

We have fabricated and characterized the principal thermal properties of a mechanically suspended nanostructure, consisting of a micron-scale suspended GaAs island, upon which we have defined superconductor-insulator-normal metal tunnel junctions. The tunnel junctions allow for sensitive thermometry and heating of the electrons in a thermally isolated normal metal element, permitting the determination of the low-temperature thermal conductance of the legs that support the GaAs island, as well as the low-temperature electron-phonon coupling. This device forms the basis of a nanoscale bolometric detector, whose optical performance can be estimated from these measurements. © 2002 American Institute of Physics. [DOI: 10.1063/1.1491300]

It has recently become possible to fabricate fully suspended, three-dimensional integrated devices that can be used for sensitive measurements of energy and thermal transport in nanostructures. Recent experiments have measured the low temperature thermal conductance of submicron single crystal GaAs wires,¹ in the range of 1–10 K, as well as the quantum of thermal conductance of a suspended polycrystalline silicon nitride membrane,² in the range of 0.1–10 K. A challenging problem is temperature measurement of the suspended device. Tighe *et al.*¹ relied on the temperature dependence of the zero-bias resistance of an n^+ -doped GaAs resistor, while Schwab *et al.*² used a dc superconducting quantum interference device to monitor the Johnson–Nyquist noise in a normal metal film. An alternate approach is to employ a superconductor-insulator-normal metal (SIN) tunnel junction as an electron thermometer. These have been used for measuring the thermal conductivity of large-scale suspended silicon nitride membranes,³ as well as for electronic refrigeration.^{4–6} SIN tunnel junctions have also been used as sensitive probes of the electron energy distribution in mesoscopic metallic systems.⁷ Here we demonstrate the integration of SIN tunnel junctions with a nanoscale suspended single-crystal GaAs structure, allowing us to measure the electron-phonon coupling in a normal metal film on the suspended structure, as well as measure the phonon thermal conductance through the supporting legs. Our device can be applied to infrared bolometry.

The device was fabricated from a GaAs/AlGaAs heterostructure consisting of a 200 nm GaAs top layer and a 400 nm $\text{Al}_{0.7}\text{Ga}_{0.3}\text{As}$ sacrificial layer, on a bulk GaAs substrate. The lateral dimensions of the mechanical structure were defined using electron-beam lithography to pattern an etch mask, used for a timed anisotropic reactive ion etch of the GaAs heterostructure. We used SiCl_4 , flowing at 10 sccm at a pressure of 3 mTorr, with a rf power of 100 W, to etch to a depth of 400 nm. The structure is shown in Fig. 1; the six supporting legs are $0.2 \times 0.2 \times 3 \mu\text{m}^3$ and the central GaAs island is $0.2 \times 5 \times 6 \mu\text{m}^3$. The AlGaAs layer was removed

with a timed wet etch in 7% hydrofluoric acid, undercutting the island and six legs. The tunnel junction circuit was defined on the surface of the suspended structure, using a second step of electron-beam lithography to create a stencil mask for angled shadow evaporation. These included a pair of SIN tunnel junctions connected back-to-back in a SINIS pair configuration, and a separate SINIS pair with two ohmic superconductor-normal metal (SN) contacts to the center normal metal element. The tunnel junctions were made by first evaporating 100 Å of Al, perpendicular to the sample surface, and oxidizing in 200 mTorr of O_2 for 3 min, forming the superconducting-insulating connections for the SIN junctions; the oxidation time determines the normal state junction resistance (R_N). A second evaporation of 100 Å of Al, at 45° to the sample surface, formed the superconducting connections for the SN contacts. A final evaporation at -45° of 600 Å of Cu completed the tunnel junctions. Only (superconducting) Al was deposited on the support legs, minimizing the thermal conductance (see Fig. 1). The tunnel junctions can

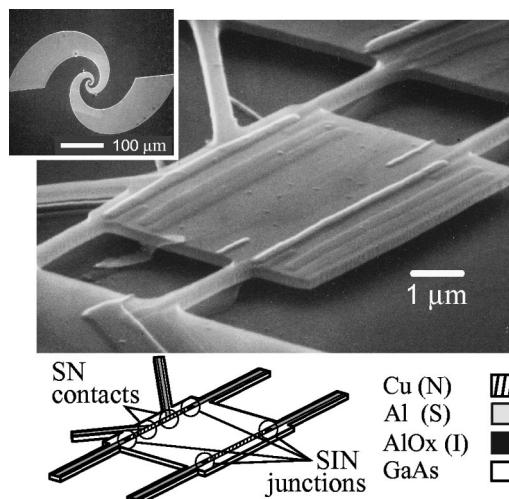


FIG. 1. Micrograph of suspended structure, with 1 μm scale bar. Top left: Log spiral antenna for coupling radiation to the device. Bottom: Schematic of device, indicating the GaAs suspended island, the six supporting legs, the SIN tunnel junctions and the ohmic SN contacts.

^{a)}Electronic mail: cleland@quest.ucsb.edu

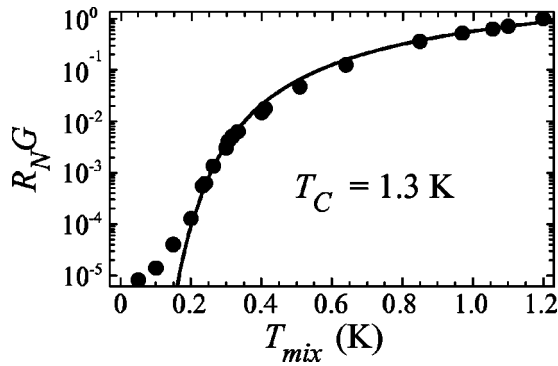


FIG. 2. Normalized zero-bias conductance G of one SNIS tunnel junction, as a function of T_{mix} . Conductance is in units of the normal state resistance R_N , and T_{mix} was measured by a calibrated thermometer. Solid line is a BCS fit to the data.

be used as SINIS junction pairs, or, using the SN contacts, as single SNIS junctions.

Electrical contacts to the device were made with Au wire bonds. The device was mounted in a stainless steel can thermally anchored to the mixing chamber of a dilution refrigerator, with a base temperature of 25 mK. All electrical connections to the sample were extensively filtered at room temperature, at the 1 K pot, and at the mixing chamber with π filters, three pole RC filters and stainless steel powder filters.

We calibrated the SINIS junction pairs as electron thermometers by measuring the zero-bias conductance $G = dI/dV(V_{\text{dc}}=0)$ as a function of the mixing chamber temperature T_{mix} . Figure 2 shows the measured normalized conductance $R_N G$ of one of the SNIS pairs, with $R_N = 20$ k Ω . The other SINIS pair was very similar, with $R_N = 130$ k Ω . Also shown is a one-parameter fit to Bardeen–Cooper–Schrieffer (BCS) theory,⁸ giving a transition temperature of $T_c = 1.3$ K, that of bulk aluminum. Measurements below 0.2 K deviate from the BCS theory, possibly due to multiple Andreev reflections in the normal section of the SINIS pair,⁹ or an indication of sufficient spurious radiation that the electrons do not cool to below 150 mK, due to the small volume of Cu ($\Omega = 6 \times 0.3 \times 0.06$ μm^3 of Cu). Bulk electron-phonon coupling theory indicates that for this volume, an ambient power of 10^{-14} W is sufficient to heat the electrons to $T_{el} = 150$ mK, for an island phonon temperature $T_{\text{island}} \approx T_{\text{mix}} = 25$ mK.¹⁰ We note that the measurement-induced heating of the electron gas is negligible, as measurements were done with an applied power of only $\approx 10^{-17}$ W.

We measured the electron-phonon coupling by passing a dc current through the two SN contacts, heating the normal metal, and monitoring the electron temperature T_{el} using one of the SNIS junctions, as shown in the inset of Fig. 3. The SIN junction, located 5 μm from the dc injection point, is ac biased to allow a lock-in measurement of the zero-bias conductance extracting T_{el} from the fit in Fig. 2. Negligible measurement power was dissipated. Figure 3 shows T_{el} as a function of power P , for different mixing chamber temperatures T_{mix} . The solid lines are fits of the form $P = \Sigma \Omega (T_{el}^n - T_{\text{island}}^n)$, with $n = 4.84$ and $\Sigma = 2 \times 10^9$ W/m³ K^{4.84}, for $T_{\text{mix}} = 25$ mK, in agreement with previous measurements;^{10–12} bulk theory predicts $n = 5$ and $\Sigma \approx 0.2 - 2 \times 10^9$ W/m³ K⁵. Measurements at other T_{mix} yield

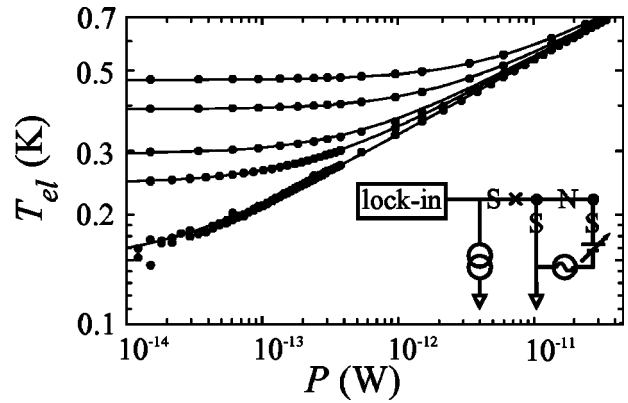


FIG. 3. Electron temperature T_{el} measured as a function of power P dissipated in the normal metal, measured at $T_{\text{mix}} = 0.025, 0.24, 0.3, 0.4,$ and 0.5 K (indicated by the intercept). The 0.025 K data intercept T_{el} at 0.15 K; solid lines are fits to the data. Inset is a diagram of the measurement setup.

similar values for n and Σ . Calculations of the acoustic mismatch¹³ between the Cu (T_{latt}) and the GaAs (T_{island}) phonon gases predict $T_{\text{latt}} > T_{\text{island}}$, which results in a reduced fit value n . However, the applicability of acoustic mismatch theory is debatable, as the phonon modes in the Cu film are effectively two-dimensional below 1 K.¹⁴ Note that we will identify the island phonon temperature T_{island} with T_{mix} .

The thermal conductance of the support legs was measured by dc biasing one of the SINIS pairs, and measuring the corresponding rise in T_{island} using an electrically isolated SNIS junction. The heating power deposited in the normal Cu section (C_1) of the first SINIS pair (see inset of Fig. 4) heats the island phonon gas, and is then transmitted through the legs to the bulk substrate. The power dissipated is $P = I(V - 2\Delta/e)$, using the measured current I and voltage V across the heater SINIS pair, assuming quasiparticle relaxation to the gap ($\Delta = 180$ μeV) as the dominant heating process, with negligible subsequent recombination.¹⁵ T_{island} is inferred from the electron temperature of the normal Cu section (C_2) of the SNIS thermometer, using the previously determined electron-phonon coupling. The measured thermal conductance is shown in Fig. 4, for $T_{\text{mix}} = 25$ and 50 mK. The solid line is a fit to the data of the form $P = \alpha(T_{\text{island}}^4$

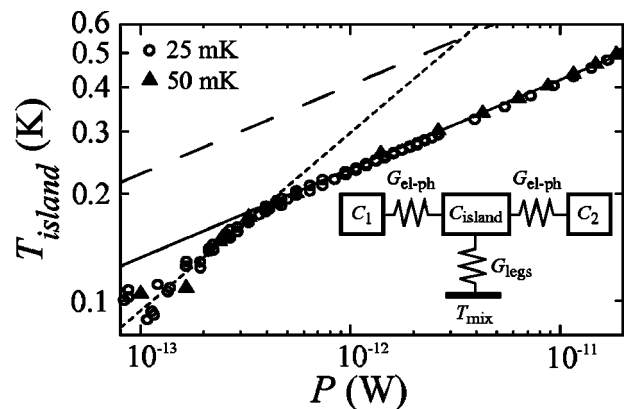


FIG. 4. Island temperature T_{island} as a function of power P dissipated in the island phonon gas, measured at $T_{\text{mix}} = 25$ mK (circles) and 50 mK (triangles). Solid line is a fit to the data, yielding a phonon mean free path $\Lambda = 7.7$ μm . The long dash line is for $\Lambda = 1$ μm , for comparison. The quantum of thermal conductance for six legs is indicated by the short dash line.

$-T_{\text{mix}}^4$) with $\alpha = 3.3 \times 10^{-10} \text{ W/K}^4$. This corresponds to a mean free path $\Lambda = 7.7 \mu\text{m}$,¹⁶ indicating that the phonons undergo primarily specular (rather than diffuse) reflections within the legs.¹ Also plotted (short dashes) is the quantum of thermal conductance^{2,17} for six legs, $6 \times 4 \times G_0 = 8\pi^2 k_B^2 T/h$. The data agree well with the bulk theory, crossing over to the quantum limit at $\sim 170 \text{ mK}$. Note the large phonon mean free path in our device masks the transition to the quantum limit; we have also plotted the bulk thermal conductance for $\Lambda = 1 \mu\text{m}$ (long dashes), which would make the transition to the quantum limit at 550 mK . In addition, the thermal conductance of the legs is significantly larger than the electron-phonon effective conductance, so the assumption that $T_{\text{island}} \approx T_{\text{mix}}$ in the electron-phonon heating measurements is a good one.

We can estimate the performance of this device as a bolometric detector, assuming an operational temperature of 100 mK . Antenna-coupled infrared power heats the electrons in C_2 , through the two SN contacts, and the resulting temperature rise in C_1 is detected with a SINIS pair (see Fig. 4). We take the electron heat capacitances $C_1 = C_2 \approx 7.4 \times 10^{-19} \text{ J/K}$ at $T = 0.1 \text{ K}$,¹⁸ and for the island phonons $C_{\text{island}} \approx 1.0 \times 10^{-20} \text{ J/K}$. The thermal conductance between the electrons in C_1 and C_2 and the island phonons is $G_{el-ph} \approx 1.1 \times 10^{-14} \text{ W/K}$, and the phonon thermal conductance of the support legs is $G_{\text{legs}} \approx 1.5 \times 10^{-13} \text{ W/K}$. The dominant thermal noise source is due to the finite value of G_{el-ph} . The estimated noise equivalent power (NEP) at low frequencies is $\text{NEP} = (4k_B T^2 G_{el-ph})^{1/2} \approx 7 \times 10^{-20} \text{ W/Hz}^{1/2}$. Current noise from the first-stage amplifier is a significant additional contribution for this device, due to the high zero-bias resistance $\sim 10^8 \Omega$, limiting the effective NEP to $\approx 4 \times 10^{-17} \text{ W/Hz}^{1/2}$.¹⁹ We are investigating alternative ap-

proaches to reading out the device, using a single-electron transistor as a first-stage amplifier.

The authors acknowledge the financial support provided by NASA Office of Space Science under Grant No. NAG5-8669 and the Army Research Office under Award No. DAAD-19-99-1-0226. We thank Bob Hill for processing support.

¹T. S. Tighe, J. M. Worlock, and M. L. Roukes, Appl. Phys. Lett. **70**, 2687 (1997).

²K. C. Schwab, E. A. Henriksen, J. M. Worlock, and M. L. Roukes, Nature (London) **404**, 974 (2000).

³M. M. Leivo and J. P. Pekola, Appl. Phys. Lett. **72**, 1305 (1998).

⁴M. Nahum, T. M. Eiles, and J. M. Martinis, Appl. Phys. Lett. **65**, 3123 (1994).

⁵M. M. Leivo, J. P. Pekola, and D. V. Averin, Appl. Phys. Lett. **68**, 1996 (1996).

⁶J. P. Pekola, A. J. Manninen, M. M. Leivo, K. Arutyunov, J. K. Suoknuuti, T. I. Suppala, and B. Collaudin, Physica B **280**, 485 (2000).

⁷H. Pothier, S. Guéron, N. O. Birge, D. Esteve, and M. H. Devoret, Phys. Rev. Lett. **79**, 3490 (1997).

⁸L. Solymar, *Superconductive Tunnelling and Applications* (Chapman and Hall, London, 1972).

⁹A. F. Volkov, A. V. Zaitsev, and T. M. Klapwijk, Physica C **210**, 21 (1993).

¹⁰F. C. Wellstood, C. Urbina, and J. Clarke, Phys. Rev. B **49**, 5942 (1994).

¹¹M. L. Roukes, M. R. Freeman, R. S. Germain, R. C. Richardson, and M. B. Ketchen, Phys. Rev. Lett. **55**, 422 (1985).

¹²A. H. Steinbach, J. M. Martinis, and M. H. Devoret, Phys. Rev. Lett. **76**, 3806 (1994).

¹³E. T. Swartz and R. O. Pohl, Rev. Mod. Phys. **61**, 605 (1989).

¹⁴ $T \approx \pi v_s \hbar / (k_B d) \approx 1.4 \text{ K}$ for $v_s = 3710 \text{ m/s}$ and $d = 60 \text{ nm}$.

¹⁵H. Kinder, Phys. Rev. Lett. **28**, 1564 (1972).

¹⁶Using $\kappa = 1/3c v_s \Lambda$, with $v_s = 3710 \text{ m/s}$ and a Debye temperature of 345 K . We note Λ is longer than the legs.

¹⁷L. G. C. Rego and G. Kirczenow, Phys. Rev. Lett. **81**, 232 (1998).

¹⁸Estimated from the specific heat of Cu.

¹⁹Estimated from the voltage responsivity of 0.4 mV/K and a current noise of $10^{-15} \text{ A/Hz}^{1/2}$.